horticulturae

MDPI

Article

Molecular Cloning and Expression Analysis of Geranyllinalool Synthase Gene (*SgGES*) from *Salvia guaranitica* Plants

Ahmed Ali Abdelhameed [1], Mohamed A. Eissa [2,3], Ragab I. El-kholy [4], Doaa Bahaa Eldin Darwish [5], Amany H. A. Abeed [6], Fathia A. Soudy [7], Amal Ahmed Alyamani [8], Hala M. Abdelmigid [8], Maissa M. Morsi [9], Jian Zhao [10,11,*], Mohammed Ali [12,*] and Muhammad Zayed [13]

1 Agricultural Botany Department (Genetics), Faculty of Agriculture, Al-Azhar University, Assuit Branch, Assuit 71524, Egypt; genetic800@gmail.com
2 Biotechnology Department, Faculty of Agriculture, Al-Azhar University, Cairo 11754, Egypt; ma.eissa@azhar.edu.eg
3 Zhejiang BioAsia Institute of Life Sciences, Pinghu 314200, China
4 Agricultural Botany (Genetics) Department, Faculty of Agriculture, Al-Azhar University, Cairo 11884, Egypt; ragab_elkholy@azhar.edu.eg
5 Biology Department, Faculty of Science, University of Tabuk, Tabuk 71491, Saudi Arabia; ddarwish@ut.edu.sa
6 Department of Botany & Microbiology, Faculty of Science, Assiut University, Assiut 71516, Egypt; dramany2015@aun.edu.eg
7 Genetics and Genetic Engineering Department, Faculty of Agriculture, Benha University, Moshtohor 13736, Egypt; soudy@fagr.bu.edu.eg
8 Department of Biotechnology, College of Science, Taif University, Taif 21944, Saudi Arabia; a.yamani@tu.edu.sa (A.A.A.); h.majed@tu.edu.sa (H.M.A.)
9 Department of Biology, College of Science, Taif University, Taif 21944, Saudi Arabia; m.moasa@tu.edu.sa
10 Key Laboratory of Tea Science of Ministry of Education, College of Horticulture, Hunan Agricultural University, Changsha 410128, China
11 National Research Center of Engineering and Technology for Utilization of Botanical Functional Ingredients, Hunan Agricultural University, Changsha 410128, China
12 Maryout Research Station, Genetic Resources Department, Desert Research Center, 1 Mathaf El-Matarya St., El-Matareya, Cairo 11753, Egypt
13 Department of Botany and Microbiology, Faculty of Science, Menoufia University, Shebin El-Kom 32511, Egypt; mhdzayed@science.menofia.edu.eg
* Correspondence: jianzhao@ahau.edu.cn (J.Z.); mohammedalidrc@gmail.com (M.A.); Tel.: +20-1553727631 (M.A.)

Abstract: *Salvia guaranitica* is considered one of the most significant medicinal and aromatic herbs in terms of nutritional and medical benefits due to its wealth of important active components. Among these compounds, terpenoids are the most prominent and abundant, particularly monoterpenes (C10), sesquiterpenes (C15), and diterpenes (C20). They are biologically advantageous to plants and perform a multitude of functions. The current study aimed to clone the *S. guaranitica* gene that encodes for geranyllinalool synthases (*SgGES*, EC: 4.2.3.144), with consideration for these features. The open reading frame of the 867-amino-acid protein encoded by *SgGES* consists of 2.721 base pairs. In addition, the SgGES protein has five domains that belong to the terpene synthase family, which are related to the terpene and terpenoid synthase domains. We manipulated and overexpressed the *SgGES* gene in *Nicotiana tabacum* to explore its function. When compared to the GUS control, the transgenic *N. tabacum* plants displayed an increase in leaf production and diameter when compared with the wild-type plants. Finally, analysis of transgenic plants using gas chromatography/mass spectrometry (GC-MS) showed that *SgGES* is responsible for producing various terpene species, especially diterpenes.

Keywords: *Salvia guaranitica*; geranyllinalool synthases; *Nicotiana tabacum*; cloning; molecular characterization

Citation: Abdelhameed, A.A.; Eissa, M.A.; El-kholy, R.I.; Darwish, D.B.E.; Abeed, A.H.A.; Soudy, F.A.; Alyamani, A.A.; Abdelmigid, H.M.; Morsi, M.M.; Zhao, J.; et al. Molecular Cloning and Expression Analysis of Geranyllinalool Synthase Gene (*SgGES*) from *Salvia guaranitica* Plants. *Horticulturae* **2024**, *10*, 668. https://doi.org/10.3390/horticulturae10070668

Academic Editors: Tetsuya Matsukawa and Daniela Scaccabarozzi

Received: 13 May 2024
Revised: 14 June 2024
Accepted: 17 June 2024
Published: 24 June 2024

1. Introduction

The genus *Salvia* (Lamiaceae) has more than 1000 species of woody, fragrant shrubs, some of which, like *S. przewalskii*, *S. miltiorrhiza*, *S. allagospadonopsis*, *S. aegyptiaca*, *S. officinalis*, *S. africana*, *S. splendens*, and *S. japonica*, are economically significant and are globally cultivated for their numerous medicinal uses and to produce essential oils (EOs). Although a plethora of *Salvia* species can be found on Earth, the majority of them are concentrated in three distinct geographical regions: East Asia (100 species), West Asia (200 species), and Central and South America (500 species). In contrast, the remaining species of *Salvia* are dispersed throughout the remainder of the world [1–4].

In recent years, EOs from *Salvia* species have emerged as a critical resource in pharmacological and aromatic research, focusing on the discovery and characterization of bioactive compounds. The essential oils derived from *Salvia* display significant bioactivities, including choleretic effects, antioxidant properties, antibacterial activity, anticancer properties, antimutagenic effects, and anti-inflammatory capabilities [5–7]. Terpenoids have been classified as the largest class of secondary metabolites and natural products. They were detected in both plants and other species, with over 40,000 unique structural variations present [2,4,8–10]. Isopentenyl diphosphate (IPP), which consists of five carbon atoms (C5), serves as the structural basis for terpenoid compounds; see Figure 1 [11,12]. The original names of these compounds were derived from the *Pistacia terebinthus* tree, which was the source from which all these unique terpene chemicals were first identified. Ruzicka and Wallach altered and depicted the structure of the terpene unit [13–16]. Certain terpenes play a vital role in the fundamental metabolic processes of plants and are indispensable for plant growth, flowering, and development. Examples of such terpenes include carotenoid pigments, the phytol side chains of chlorophyll, phytohormones, and certain constituents of cellular membranes [17,18]. Nonetheless, most terpenes that have been discovered are classified as secondary metabolites and are crucial to the way plants interact with their natural environments. Terpenes, both volatile and nonvolatile, are known to play a significant role in the defense against insects and microbes, as well as in the attraction of pollinators and the management of photo-oxidative stress [19]. To gain a comprehensive understanding of the functions of terpenes and terpenoid compounds, extensive research is currently being conducted [2,4,9,10,20,21]. *Salvia* species are widely recognized for their significant concentration of EOs, with mono- and sesquiterpenes constituting most of the constituents of their fragrant essential oils [2,22–28]. According to [4], the primary sesquiterpenes in the Chinese cultivar of *S. guaranitica* are germacrene-A, isocaryophyllene, germacrene-C, humulene, caryophyllene, germacrene-D, pi-a-murolene, caryophyllene oxide, and d-cadinene. The pharmacological and physiological roles of these sesquiterpenes are diverse, and many of the genes responsible for synthesizing these compounds in *Salvia* are yet to be identified. In this study, the gene encoding the geranyllinalool synthase (*SgGES*, EC: 4.2.3.144) enzyme from *S. guaranitica* was cloned and subsequently subjected to functional characterization. Additionally, the recombinant *SgGES* catalyzed the conversion of geranylgeranyl diphosphate (GGPP) into a range of terpene products, including diterpenes in various forms.

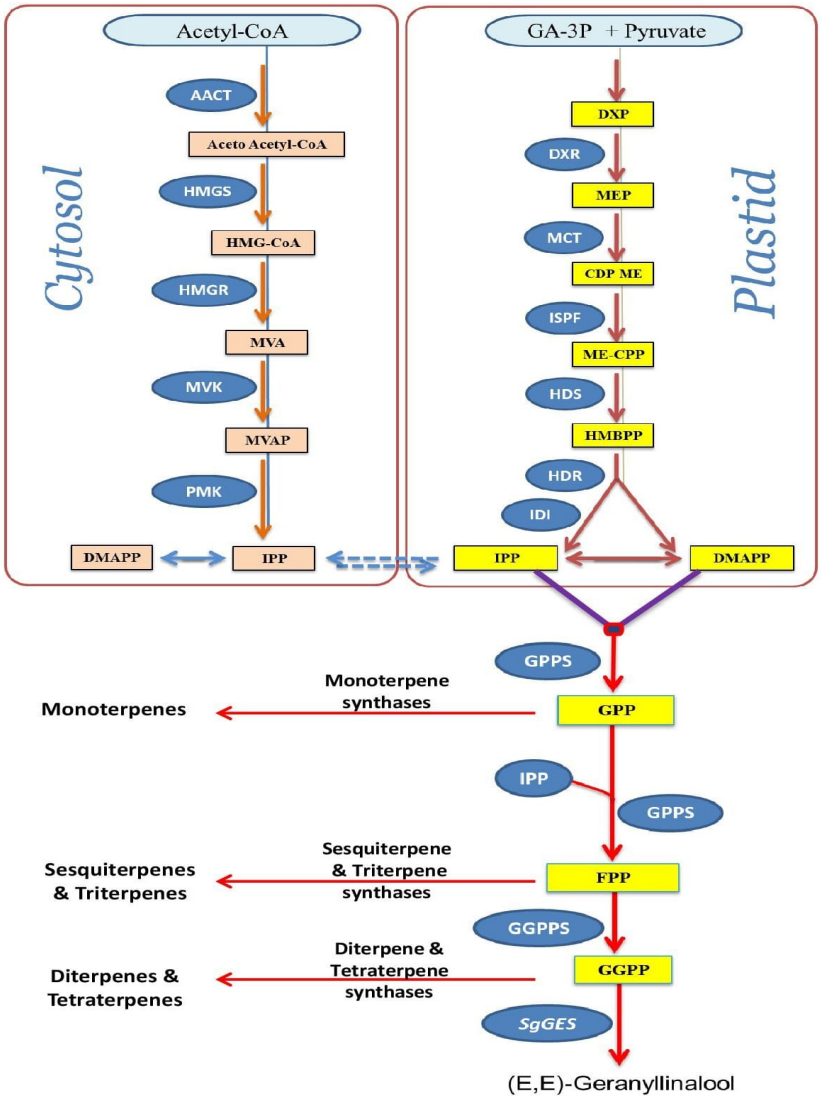

Figure 1. Biosynthetic pathways for production of (E,E)-geranyllinalool synthase and other terpenoids. DXS: 1-deoxy-D-xylulose-5- phosphate synthase, DXR: 1-deoxy-D-xylulose-5-phosphate reductoisomerase, MCT: 2-C-methyl-D-erythritol 4-phosphate cytidylyltransferase, ISPF: 2-C-methyl-D-erythritol 2,4-cyclodiphos-phate synthase, HDS: (E)-4-hydroxy-3-methylbut-2-enyl-diphosphate synthase, HDR: 4-hydroxy-3-methylbut-2-enyl diphosphate reductases, IDI: isopentenyl-diphosphate delta isomerase, AACT: acetyl-CoA C-acetyl transferase, HMGS: hydroxyl methyl glutaryl-CoA synthase, HMGR: hydroxymethyl glutaryl-CoA reductase (NADPH), MVK: mevalonate kinase, PMK: phospho-mevalonate kinase, GPPS: geranyl pyrophosphate synthase, FPPS: farnesyl pyrophosphate synthase, GGPS: geranylgeranyl pyrophosphate synthase.

2. Materials and Methods

2.1. Plant Materials

S. guaranitica plantlets were collected from the Wuhan Botanical Garden (WBG), Chinese Academy of Sciences, located in Hubei, Wuhan, China. Following that, the plantlets were cultivated in the greenhouse of the National Research Centre in Cairo, Egypt. Young leaves from five-year-old plants were collected and rapidly frozen in liquid nitrogen for 15 min and stored at −80 °C to isolate RNA and prepare for gene cloning.

2.2. Sequence Characterization of SgGES

The sequence of the *SgGES* gene was selected based on the highest sequence similarity it displayed when compared with genes responsible for plant diterpene synthesis that are

already known. The PROTPARAM server (http://web.expasy.org/protparam/, accessed on 15 January 2024) was utilized to evaluate the physical and chemical characteristics of *SgGES*. We employed the iPSORT prediction tool (http://ipsort.hgc.jp/, accessed on 16 June 2024) to analyze the putative transit peptide for open reading frames (ORFs) of *SgGES*. To compare and analyze the sequence of *SgGES* with known proteins, we used the NCBI BLASTX tool (http://blast.ncbi.nlm.nih.gov/, accessed on 5 June 2023). The PhyML Server aided the understanding of the evolutionary relationships of the *SgGES* protein and other plant TPS proteins between the *SgGES* protein and other plant TPS proteins, without requiring any adjustments to the parameters of the tool (http://www.phylogeny.fr/, accessed on 16 June 2024) [2,4,29,30]. Moreover, PROTPARAM software (http://web.expasy.org/protparam, accessed on 15 May 2023) facilitated the determination of the physiochemical properties of *SgGES*.

2.3. Putative Tissue Expression Pattern and Subcellular Localization of SgGES

Based on the *Arabidopsis* eFP browsers (http://bar.utoronto.ca/efp/cgi-bin/efpWeb.cgi, accessed on 16 June 2024), tissue-specific expression data from seventy-two (e.g., Dry seed, Imbibed seed, 24 h, 1st Node, Flower Stage 12, Stamens, Cauline Leaf, Cotyledon, Root, Entire Rosette After Transition to Flowering, Flower Stage 9, Flower Stage 10/11, Flower Stage 12, Flower Stage 15, Flower Stage 12, Carpels, Flower Stage 12, Petals, Flower Stage 12, Sepals, Flower Stage 15, Carpels, Flower Stage 15, Petals, Flower Stage 15, Sepals, Flower Stage 15, Stamen, Flowers Stage 15, Pedicels, Leaf 1 + 2, Leaf 7, Petiole, Leaf 7, Distal Half, Leaf 7, Proximal Half, Hypocotyl, Root, Rosette Leaf 2, Rosette Leaf 4, Rosette Leaf 6, Rosette Leaf 8, Rosette Leaf 10, Rosette Leaf 12, Senescing Leaf, Shoot Apex, Inflorescence, Shoot Apex, Transition, Shoot Apex, Vegetative, Stem, 2nd Internode, Mature Pollen, Seeds Stage 3 w/Siliques, Seeds Stage 4 w/Siliques, Seeds Stage 5 w/Siliques, Seeds Stage 6 w/o Siliques, Seeds Stage 7 w/o Siliques, Seeds Stage 8 w/o Siliques, Seeds Stage 9 w/o Siliques, Seeds Stage 10 w/o Siliques, Vegetative Rosette, Globular—apical, Globular—basal, Heart—cotyledons, Heart—root, Torpedo—cotyledons, Torpedo—apical, Torpedo—root, Torpedo—basal, Torpedo—meristem, cross-section of leaf/mesophyll cells no ABA, cross-section of leaf/mesophyll cells with 100 µM ABA, surface view of leaf/guard cells no ABA, surface view of leaf/guard cells with 100 µM ABA, mesophyll cells without ABA/cordycepin and actinomycin added during protoplasting, mesophyll cells without ABA/no cordycepin nor actinomycin, mesophyll cells with 100 µM ABA/cordycepin and actinomycin added during protoplasting, mesophyll cells with 100 µM ABA/no cordycepin nor actinomycin, guard cells without ABA/cordycepin and actinomycin added during protoplasting, guard cells without ABA/no cordycepin nor actinomycin, guard cells with 100 µM ABA/cordycepin and actinomycin added during protoplasting, guard cells with 100 µM ABA/no cordycepin nor actinomycin, stem epidermis/top of stem, whole stem/top of stem, stem epidermis/bottom of stem, and whole stem/bottom of stem; see Supplementary Materials Table S1) tissues were analyzed to generate expression profiles. The putative sub-cellular localizations of the *SgGES* gene was analyzed using the Cell-eFP browsers (http://bar.utoronto.ca/cell_efp/cgi-bin/cell_efp.cgi, accessed on 16 June 2024) [31,32]. The color boxes represent the expression scale (e.g., red color—high expression and yellow color—low expression).

2.4. RNA Extraction and cDNA Synthesis

Six tissues from five-year-old *S. guaranitica* were used to extract RNA using TransZol Reagent (Invitrogen, Carlsbad, CA, USA). Also, RNA was extracted from leaves of wild-type and transgenic *N. tabacum* for semi-quantitative RT-PCR (sqRT-PCR). For cDNA synthesis, 1 µg of RNAs was used to synthesize the first-strand cDNA using TransScript® First-Strand cDNA Synthesis Super Mix kit (Invitrogen, Carlsbad, CA, USA), as described by the authors of [2,33].

2.5. Isolating the Full-Length SgGES Gene

The complete *SgGES* cDNA was used as a template to amplify the full-length gene using short gene-specific forward (5′-ATGATAAACATTATGTATACAAGCTAGCC-3′) and reverse (5′-CTAATTAAGGAAA AGTGAGAAACAAACAC-3′) primers and TaKaRa Taq DNA Polymerase enzyme (TaKaRa, Beijing, China). The amplification conditions were 4 min at 96 °C; 33 cycles for 13 s at 96 °C; 30 s at 58 °C; 96 s at 68 °C; and then 14 min at 68 °C. The first PCR product was used as a template for the second PCR using long gene-specific forward (5′-GGGGACAAGTTTGTACAAAAAAGCAGGCTTC ATGATAAACATTATGTAT-3′) and reverse (5′-GGGGACCACTTTGTACAAGAAAGCTGGGTAAAGTGAGAAACAAACAC-3′) primers. We adopted the same polymerase enzyme and PCR program. The amplicon was cloned into a pDONR-221 vector (Invitrogen, Carlsbad, CA, USA) and then pB2GW7 vector with the cauliflower mosaic virus (CaMV) 35S promoter as a strong constitutive promoter (Invitrogen, Carlsbad, CA, USA) and sequenced as described by the authors of [2,4].

2.6. Nicotiana Tabacum Leaf Transformation Procedure Using Plant Tissue Culture Method and Preparation of Agrobacterium Cultures for Infection

To ensure that *SgGES* is consistently expressed in tobacco plants, we utilized the *Agrobacterium tumefaciens* strain GV3101 to infect *N. tabacum* leaves. The pB2GW7-SgGES vector was introduced into the *A. tumefaciens* strain GV3101 by the direct electroporation method. This strain carried the construct plasmid pB2GW7-SgGES, and the expression of our target gene in this plasmid was driven by the 35S promoter (see Supplementary Materials Figure S1). Utilizing leaf discs from tobacco, a slightly modified protocol was implemented that was originally described by the authors of [2,34–36]. Transgenic tobacco plants were regenerated, and then the positive transgenic plantlets were selected with 55 mg/L hygromycin. More than 10 individual transgenic tobacco lines were generated and examined with RT-PCR for positive transgenic lines. Transgenic plants with good and healthy roots were transferred to the greenhouse for acclimatization. To facilitate this, the transgenic plants were provided with regular watering and fertilization using Miracle-Gro fertilizer (Scott's Company, Marysville, OH, USA). Plants were grown in growth chambers with a temperature of 22 °C during the day and 20 °C at night and a humidity of 60–70%. The photoperiod was set at 16 h during the day and 8 h at night, and the light density was 100–150 μ moles m^{-2} s^{-1}, with fluorescent bulbs used for flowering and vegetative growth. Finally, the transgenic tobacco and control plants were analyzed for growth, leaf morphology, and terpenoid profiling.

2.7. Semi-Quantitative RT-PCR (sqRT-PCR) Analysis

To confirm the gene transfer process, sqRT-PCR was conducted using a PCR system from Biometra (Biometra, Jena, Germany). The NtEF-1α gene was utilized as a housekeeping gene (forward primer 5′-TGGTTGTGACTTTTGGTCCCA-3′; reverse primer 5′-ACAAACCCACGCTTGAGATCC-3′) with a length of 155 base pairs, while the *SgGES* gene was amplified using the forward primer 5′-CATGGTGTGTACCCTGTTAG-3′ and reverse primer 5′-GATCTTTGAGGCGGTAGATG-3′, with a length of 159 base pairs. The primers for our study were designed using the online platform provided by IDTdna (http://www.idtdna.com/scitools/Applications/RealTimePCR/, accessed on 16 June 2024). The sqRT-PCR reaction was carried out utilizing the Biometra Thermocycler T-Gradient Thermo Block system, with the program executed as follows: an initial denaturation phase at 94 °C for 5 min, followed by 33 cycles of denaturation at 96 °C for 34 s, annealing at 59 °C for 30 s, and extension at 72 °C for 1.3 min. The final extension phase was carried out at 72 °C for 10 min. The PCR products were then analyzed on a 1.35% agarose gel to assess gene expression levels.

2.8. Terpenoid Extraction and GC-MS Analysis

Intact leaves from both transgenic and non-transgenic *N. tabacum* plant lines were frozen in liquid nitrogen (LN2) and subsequently crushed using a ceramic mortar and pestle before being immersed in the solvent n-hexane for 73 h. This process ensures the complete extraction of terpenoids from the leaves, as previously described [2,9,10,20,21]. An approximately 1 µL aliquot of each extract from a 1.5 mL crimp vial was analyzed using the Shimadzu GC-MS system (Tokyo, Japan) with three technical replicates. The analysis was performed by the Wiley GC/MS Library, the Volatile Organic Compounds (VOCs) Analysis S/W software https://www.intertek.com/chemicals/voc-testing/, accessed on 16 June 2024, and the NIST Library, which was utilized as a reference to identify terpenoids according to previously described methods [2,4].

2.9. Quantitative Real-Time PCR (qRT-PCR) Analyses

qRT-PCR was employed to determine the quantity of *SgGES* transcripts responsible for the synthesis of geranyllinalool synthases. For this purpose, tissue samples were obtained from various plant parts, including flowers, flowering buds, roots, stems, young leaves, and old leaves. A total of three biological replicates were collected for each sample type. The housekeeping gene used in this reaction was *SgACTIN*. Its forward primer was 5′-CTGGATTTGCGGGAGATG-3′, and its reverse primer was 5′ CCGTGCTCAATTGGATACTT-3′. For *SgGES*, the forward primer used was 5′-GTAACTCGCATCGCACAT-3′, and the reverse primer used was 5-GAAGCAAGAGACGCTATCAG-3. The qRT-PCR reaction was carried out using an IQTM5 System, SYBR Green. The program was modified to include the following settings: 94 °C for 12 s, 59 °C for 30 s, and 72 °C for 22 s, followed by 65 °C for 6 s and 93 °C for 6 s. The expression levels were calculated by comparing our target gene cycle thresholds (CTs) with the housekeeping gene *SgACTIN* using the $2^{-\Delta\Delta Ct}$ method [33,37–39]. Values are reported as the means ± SE from three independent RNA pool replicates.

3. Results

3.1. Full-Length Geranyllinalool Synthase (SgGES) Clone and Sequence Analysis

The open reading frame (ORF) of the *SgGES* gene spans a length of 2721 base pairs and is responsible for encoding a protein consisting of 867 amino acids. This protein has a predicted instability index of approximately 45.48, a theoretical isoelectric point (pI) of 9.54, an aliphatic index of 94.94, a grand average of hydropathicity (GRAVY) of −0.037, a molecular mass of 100.172 kilodaltons (kDa), and a total of 56 negatively charged residues (Asp + Glu) and 101 positively charged residues (Arg + Lys). The N-terminal region of *SgGES* is composed of a thirty-amino-acid peptide (MINIMYTSPTLGDFHESKRWQNNIS-NYTYI), which forms a lengthy signal peptide, comparable to the monoterpene synthases (600–650 aa) and sesquiterpene synthases (550–580 aa). Moreover, this signal peptide in N-terminus was used as an intracellular postal code for the targeting of the protein to secretory pathways, such as cell membranes or chloroplasts. The 'iPSORT' program has revealed that *SgGES* is in either the chloroplast or the mitochondria, where the biosynthesis of farnesyl diphosphate (FPP) occurs.

NCBI-BLASTx analysis, depicted in Table 1, revealed that *SgGES* exhibited varying levels of identity with its homologous diterpene synthase proteins from various plants, including *Salvia splendens* (98.54%), *Salvia hispanica* (87.44%), *Salvia miltiorrhiza* (74.76%), and others. The *SgGES* gene sequence alignment with known and putative TPS genes from Lamiaceae and other plants helped to predict its potential function. This prediction indicates that the *SgGES* protein contains multiple domains, as reported by the Superfamily, Pfam, and InterPro databases. As a result, the *SgGES* protein comprises five terpene synthase family (TSF) domains, which include two terpenoid cyclases/protein prenyltransferase alpha-alpha toroid domains (IPR008930/SSF48239, spanning from 35 to 133 and 235 to 440), an isoprenoid synthase domain (IPR008949/SSF48576, from 463 to 783), a terpene synthase N-terminal domain (IPR001906/PF01397, from 226 to 425), and a terpene synthase metal-binding domain (IPR005630/PF03936, from 466 to 727) (as depicted in

Figure 2). The previous domains have been widely recognized in various mono-, sesqui-, and diterpene synthases [2,4,9,10,12,40,41]. *SgGES* was classified into the TPS-a subfamily of angiosperm sesquiterpene synthases, as determined by phylogenetic analysis results (Figure 3). This subfamily is primarily responsible for synthesizing mono-, sesqui-, and diterpene synthases [2,4,42,43].

Table 1. BLASTX analysis *SgGES* compared with the NCBI protein database for gene identification purposes.

NCBI Accession	[a] Descriptiona	Organism	*E* Value	Max Score	Total Score	Query Cover	Identity (%)	Accession Length
XP_042043873.1	(E,E)-geranyllinalool synthase-like	*Salvia splendens*	0.0	1582	1582	90%	98.54%	837
XP_041991789.1	(E,E)-geranyllinalool synthase-like	*Salvia splendens*	0.0	1575	1575	90%	98.18%	837
XP_047940334.1	(E,E)-geranyllinalool synthase-like	*Salvia hispanica*	0.0	1526	1526	90%	94.66%	834
XP_041994219.1	(E,E)-geranyllinalool synthase-like	*Salvia splendens*	0.0	1435	1435	90%	87.90%	851
XP_047964745.1	(E,E)-geranyllinalool synthase-like	*Salvia hispanica*	0.0	1414	1414	90%	87.44%	850
XP_057764549.1	S-linalool synthase	*Salvia miltiorrhiza*	0.0	1184	1184	90%	74.76%	820
QEV81852.1	Terpene synthase 13	*Prunella vulgaris*	0.0	1067	1067	90%	66.07%	881
PIN19742.1	Alpha-farnesene synthase	*Handroanthus impetiginosus*	0.0	993	993	90%	60.83%	846
UVE15964.1	Geranyllinalool synthase	*Leonurus japonicus*	0.0	989	989	84%	64.99%	827
QIQ55998.1	Putative terpene synthase 7	*Eremophila drummondii*	0.0	872	872	83%	59.04%	792

[a] Description—homology search using BLASTX.

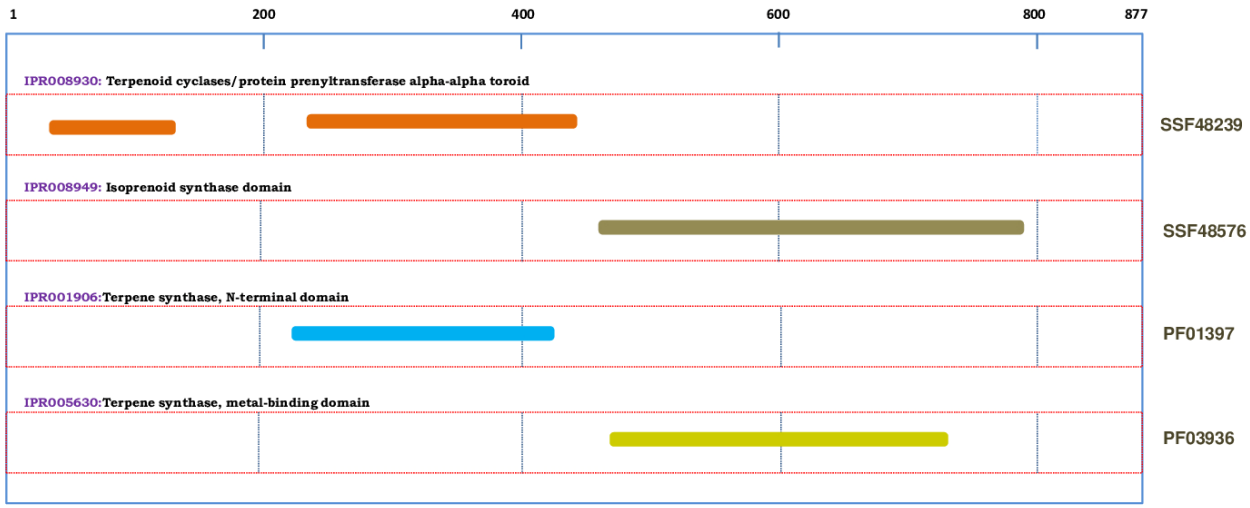

Figure 2. Putative domain analysis for SgGES using the InterPro protein sequence analysis and classification (https://www.ebi.ac.uk/interpro/ accessed on 10 July 2023) database. SgGES protein sequence has four protein family domains. Terpenoid cyclases/protein prenyltransferase alpha-alpha toroid domains (IPR008930/SSF48239, spanning from 35 to 133 and 235–440), an isoprenoid synthase domain (IPR008949/SSF48576, from 463 to 783), a terpene synthase N-terminal domain (IPR001906/PF01397, from 226 to 425), and a terpene synthase metal-binding domain (IPR005630/PF03936, from 466 to 727).

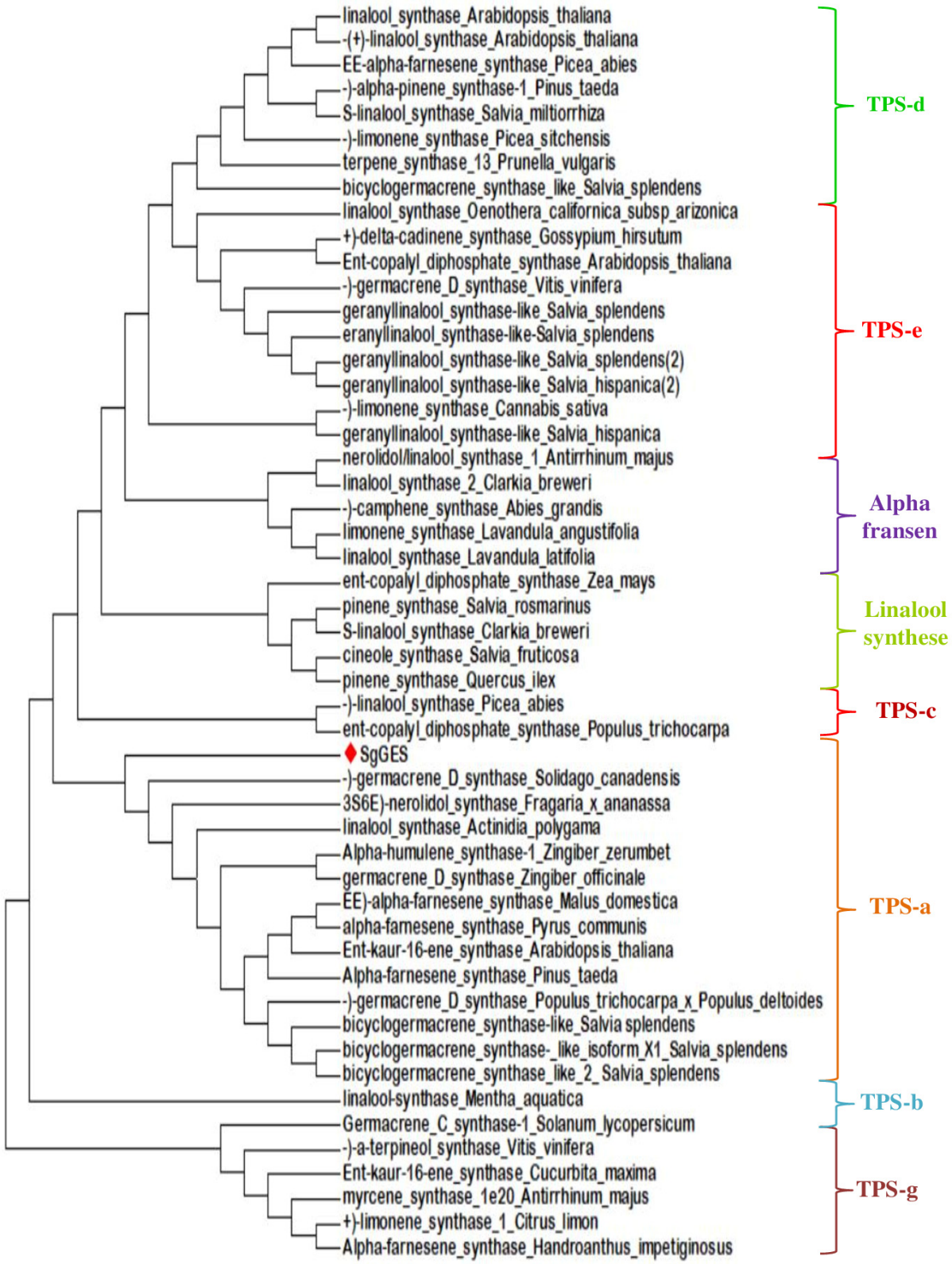

Figure 3. Phylogenetic tree of SgGES with selected terpene synthases from other plants. Seven previously identified TPS subfamilies (TPS-a to TPS-g) were chosen based on Bohlmann et al., 1998 and Ali et al., 2022 and 2021 [8–10]. The alignment was performed using the PhyML server. The numbers indicated are the actual bootstrap values of the branches.

3.2. Putative Tissue Expression and Subcellular Localization of SgGES Gene

We performed a BlastP search against *A. thaliana* genomics with the Phytozome database (https://phytozome-next.jgi.doe.gov/, accessed on 16 June 2024) to monitor the putative tissue expression pattern of *SgGES* in *A. thaliana* with the nucleotide sequence of *SgGES* as a query. As a result, several nucleotides closely related to the *SgGES* sequences, especially (AT1G61120), with high BLAST identities % and e-values (73% and 5.81^{e-4}) were identified. The tissue expression of the *SgGES* gene in *Arabidopsis* discovered by our data was analyzed across seventy-two tissues using the BAR database (http://bar.utoronto.ca/efp/cgi-bin/efpWeb.cgi, accessed on 16 June 2024) and the *Arabidopsis* Electronic Fluorescent Pictograph browsers (eFP browsers (http://bar.utoronto.ca/efp/cgi-bin/efpWeb.cgi, accessed on 16 June 2024) (Figure 4A–E). As demonstrated by the *Arabidopsis* eFP browsers, the *SgGES* gene (AT1G61120) was found in the majority of the tissues and was highly expressed in Flower Stage 15, Sepals (303.35), Flower Stage 15 (128.03), Rosette Leaf 4 (85.63), Flower Stage 12, Sepals (85.28), Leaf 7, Distal Half (58.53), Flower Stage 12 (49.55), and Rosette Leaf 6 (38.42).

Moreover, the expression of the *SgGES* (AT1G61120) gene displayed an elevated expression specifically at the embryo development stage; for example, our gene was highly expressed in Heart—cotyledons (46.13), followed by Torpedo—cotyledons (45.97), Torpedo—root (21.47), and Torpedo—basal (21.38) (Figure 4B and Supplementary Materials Table S1). On the other hand, the application of 100 µM Abscisic acid (ABA) led to an increase in the expression of the *SgGES* gene in both guard and mesophyll cells, regardless of the presence of cordycepin and actinomycin during protoplasting. In mesophyll cells treated with 100 µM ABA, cordycepin and actinomycin were added during protoplasting, resulting in a value of 154.49. This was followed by the cross-section of mesophyll cells in the presence of 100 µM ABA, which had a value of 80.39. In comparison, mesophyll cells without ABA, cordycepin, and actinomycin during protoplasting had a value of 74.61, while the cross-section of mesophyll cells without ABA had a value of 43.29 (as shown in Figure 4C and the Supplementary Materials Table S1). In addition, the *SgGES* gene was highly expressed in the stem epidermis/top of stem (9.76), followed by stem epidermis/bottom of stem (8.03), whole stem/bottom of stem (3.15), and whole stem/top of stem (2.8); see Figure 4D. Furthermore, the subcellular localization of the (*SgGES* gene: AT1G61120) gene was predicted using ePlant and cell eFP (http://bar.utoronto.ca/cell_efp/cgi-bin/cell_efp.cgi, accessed on 16 June 2024) and displayed various expression levels for 14 cell organelles, as depicted in Figure 4E.

3.3. Monitoring the Expression of SgGES Using qRT-PCR

The transcripts of *SgGES* at various tissues of *S. guaranitica* (e.g., flowering buds, flowers, roots, stems, young and old leaves) were measured using qRT-PCR. The results revealed that flowers displayed the highest expression levels of all the tissues analyzed, followed by bud flowers, young leaves, roots, old leaves, and stems (Figure 5).

3.4. Functional Expression of SgGES Gene N. tabacum Plants

We utilized *N. tabacum* plants as a transgenic expression system for conducting a further investigation on the function of the *SgGES* gene (Figure 6A). Subsequently, we confirmed the presence of positive transgenic tobacco plants using semi-quantitative RT-PCR (Figure 6B).

3.5. Phenotypic Evaluation

Comparisons of the phenotype between *N. tabacum* plants transformed with *SgGES* and their wild-type counterparts were conducted. The assessment included evaluations of leaf morphology, growth, and terpene metabolism. The transformed plants have large green oval leaves compared with the control plants (non-transformant plants), which have small green oval leaves. Moreover, the transformed plants are growing fast and have larger numbers of leaves than the control plants.

3.6. Overexpression of the SgGES Gene Altered the Terpene Profiles in Transgenic and Non-Transgenic Tobacco Plants

To explore the impact of overexpressing the *SgGES* gene on the terpene profiles of *N. tabacum* leaves, GC-MS was employed to compare the changes in metabolic profiles between transgenic plants and non-transgenic controls. The results revealed a significant increase in numerous terpenes in transgenic *N. tabacum* leaves that showed expression of the *SgGES* gene compared to the non-transgenic plants (Figure 7 and Table 2). In leaves of *N. tabacum* plants overexpressing *SgGES*, (E,E)-geranyllinalool appeared as the main diterpene compound (33.8%), followed by α-Linolenic acid (23.73%) and Palmitic acid (11.74%) as fatty acids, whereas, (+)-Ledol compounds (1.15%) and Squalene compounds (0.43%) showed up as the main sesquiterpene and triterpene compounds, respectively.

Table 2. The major terpenoid compositions in transgenic *N. tabacum* leaves over-expressing *SgGES*.

N	Compound Name	R.T (min.)	Formula	Molecular Mass (g mol^{-1})	Terpene of Type	% Peak Area	
						AtW.T	*SgTPS*-V
1	3,4-Dimethylcyclohexanol	16.114	$C_8H_{16}O$	128.212		0.04	
2	L-(-)-Nicotine	25.9	$C_{10}H_{14}N_2$	162.232		**23.06**	
3	Cycloheptasiloxane, tetradecamethyl-	29.69	$C_{14}H_{42}O_7Si_7$	519.0776			0.02
4	Trans-β-Ionone	30.644	$C_{13}H_{20}O$	192.2973			0.05
5	Topanol	31.134	$C_{15}H_{24}O$	220.3505	Sesqui	0.06	
6	Stavox	31.345	$C_{15}H_{24}O$	220.3505	Sesqui		0.15
7	Cyclooctasiloxane, hexadecamethyl-	34.574	$C_{16}H_{48}O_8Si_8$	593.2315			0.16
8	Carbamic acid, methyl-, 3-methylphenyl ester	36.029	$C_9H_{11}NO_2$	165.1891			0.06
9	Tetradecanal	37.76	$C_{14}H_{28}O$	212.3715	Fatty acids		0.09
10	Octadeamethyl-cyclononasiloxane	38.761	$C_{18}H_{54}O_9Si_9$	667.3855			0.32
11	Pentadecanoic acid	39.636	$C_{15}H_{30}O_2$	242.3975	Fatty acids		0.14
12	N-Pentadecanal	40.583	$C_{15}H_{30}O$	226.3981	Fatty acids	0.17	
13	Oxirane, tetradecyl-	40.777	$C_{16}H_{32}O$	240.4247			1.29
14	Linolenic acid;Methyl linolenate	42.253	$C_{19}H_{32}O_2$	292.4562	Fatty acids	0.86	
15	Alpha.-Linolenic acid, trimethylsilyl ester	42.458	$C_{21}H_{38}O_2Si$	350.6107	Fatty acids		0.8
16	Palmitic acid, methyl ester	43.187	$C_{17}H_{34}O_2$	270.4507	Fatty acids		0.1
17	Methyl α-linolenate	44.012	$C_{19}H_{32}O_2$	292.4562	Fatty acids		3.48
18	N-Hexadecanoic acid	44.285	$C_{16}H_{32}O_2$	256.4241	Fatty acids	4.36	
19	Palmitic acid	44.686	$C_{16}H_{32}O_2$	256.4241	Fatty acids		11.74
20	Cycloartanyl acetate	45.616	$C_{32}H_{54}O_2$	470.77		0.63	
21	Hexadecamethyl-cyclooctasioxane	45.865	$C_{16}H_{48}O_8Si_8$	593.2315			0.3
22	Labda-8,13-(E)-dien-15-ol	45.95	$C_{20}H_{34}O$	290.4834	Di		0.2
23	Stearin, 2-mono	46.238	$C_{21}H_{42}O_4$	358.5558			0.11
24	Geranylgeraniol	46.367	$C_{22}H_{36}O_2$	332.52	Di	0.35	
25	Guaia-1(10),11-diene;	46.392	$C_{15}H_{24}$	204.3511	Sesqui		0.65

Table 2. *Cont.*

N	Compound Name	R.T (min.)	Formula	Molecular Mass (g mol^{-1})	Terpene of Type	% Peak Area	
						AtW.T	*SgTPS*-V
26	All-trans-Retinol acetate	46.593	$C_{22}H_{32}O_2$	328.4883		0.55	
27	(+)-Ledol; d-Ledol	46.691	$C_{15}H_{26}O$	222.3663	Sesqui		0.63
28	Linoleic acid, methyl ester	46.888	$C_{19}H_{34}O_2$	294.4721	Fatty acids	0.11	
29	Retinol, acetate, all-trans	46.926	$C_{22}H_{32}O_2$	328.4883			0.87
30	Linolenic acid	47.041	$C_{19}H_{32}O_2$	292.4562	Fatty acids	0.47	
31	Methyl linoleate	47.192	$C_{19}H_{34}O_2$	294.4721	Di		0.45
32	Cis-Phytol	47.267	$C_{20}H_{40}O$	296.531	Di	**4.71**	
33	Farnesyl butyrate	47.341	$C_{19}H_{32}O_2$	292.4562	Di		0.74
34	Phytol	47.603	$C_{20}H_{40}O$	296.531	Di		**4.82**
35	Citronellyl geranylate	47.702	$C_{20}H_{34}O_2$	306.4828	Di	1.32	
36	(Z)-β-Elemene;	48.037	$C_{15}H_{24}$	204.3511	Di	0.27	
37	(2E,6E)-Farnesyl pentanoate	48.064	$C_{20}H_{34}O_2$	306.4828	Di		1.22
38	Phytol, trimethylsilyl ether	48.303	$C_{23}H_{48}OSi$	368.7121	Di		0.21
39	geranylgeraniol	48.418	$C_{22}H_{36}O_2$	332.52	Di		0.28
40	Linolenic acid	48.532	$C_{18}H_{30}O_2$	278.4296	Fatty acids	8.02	
41	α-Linolenic acid	48.907	$C_{18}H_{30}O_2$	278.4296	Fatty acids		23.73
42	Geranylgeraniol	48.948	$C_{22}H_{36}O_2$	332.52	Di	1.17	
43	4,8,13-Duvatriene-1,3-Diol	49.156	$C_{20}H_{34}O_2$	306.4828		0.68	
44	Stearic acid	49.281	$C_{18}H_{36}O_2$	284.4772	Fatty acid		2.86
45	(+)-Ledol	49.552	$C_{15}H_{26}O$	222.3663	Sesqui		**1.15**
46	4,8,13-Duvatriene-1,3-Diol	50.049	$C_{20}H_{34}O_2$	306.4828		43.79	
47	α-Limonene diepoxide	50.216	$C_{10}H_{16}O_2$	168.2328	Mono	0.84	
48	(E,E)-Geranyllinalool	50.461	$C_{20}H_{34}O$	290.4834	Di		**33.8**
49	Behenyl alcohol	51.405	$C_{22}H_{46}O$	326.6		0.23	
50	d-Ledol	51.493	$C_{15}H_{26}O$	222.3663	Sesqui		0.07
51	Octadeamethyl-cyclononasiloxane	52.037	$C_{18}H_{54}O_9Si_9$	667.3855			0.65
52	Methyl 11,14,17-icosatrienoate	52.978	$C_{21}H_{36}O_2$	320.5093		0.24	
53	Cyclononasiloxane, octadecamethyl-	53.436	$C_{18}H_{54}O_9Si_9$	667.3855			0.05
54	7,10-Hexadecadienoic acid, methyl ester	53.481	$C_{17}H_{30}O_2$	266.4189		0.7	
55	Squalene	54.046	$C_{30}H_{50}$	410.718	Tri		**0.43**
56	n-Heneicosane	54.964	$C_{21}H_{44}$	296.5741			0.05
57	Octadeamethyl-cyclononasiloxane	56.355	$C_{18}H_{54}O_9Si_9$	667.3855			0.79
58	Methyl linolenate, α	57.393	$C_{19}H_{32}O_2$	292.4562	Fatty acids		0.09
59	n-Pentatriacontane	58.253	$C_{35}H_{72}$	492.9462		0.52	
60	n-Pentatriacotane	58.992	$C_{35}H_{72}$	492.9462			0.79

Table 2. *Cont.*

N	Compound Name	R.T (min.)	Formula	Molecular Mass (g mol^{-1})	Terpene of Type	% Peak Area	
						AtW.T	*SgTPS*-V
61	Phthalic acid dioctyl ester	59.688	$C_{24}H_{38}O_4$	390.5561	Ester	0.49	
62	phthalic acid	60.497	$C_{24}H_{38}O_4$	390.5561	Ester		0.15
63	Methyl 11,14,17-icosatrienoate	60.973	$C_{21}H_{36}O_2$	320.5093		0.4	
64	Homomyrtenol	61.574	$C_{11}H_{18}O$	166.26	Mono		0.13
65	Octadeamethyl-cyclononasiloxane	62.682	$C_{18}H_{54}O_9Si_9$	667.3855			1.06
66	n-Heneicosane	63.222	$C_{21}H_{44}$	296.5741	Alkane	0.18	
67	n-Tetracontane	64.117	$C_{40}H_{82}$	563.0791	Alkane		0.14
68	n-Nonacosane	66.567	$C_{29}H_{60}$	408.7867	Alkane	0.09	
69	Isovaleric acid, allyl ester	68.645	$C_8H_{14}O_2$	142.1956			0.23
70	henicosane	68.682	$C_{21}H_{44}$	296.5741	Alkane	1.55	
71	Tetracontane	69.7	$C_{40}H_{82}$	563.0791	Alkane		1.61
72	Octadeamethyl-cyclononasiloxane	70.054	$C_{18}H_{54}O_9Si_9$	667.3855			1.15
73	Tetrapentacontane	71.42	$C_{54}H_{110}$	759.4512			0.03
74	9,12-Octadecadien-1-ol, (Z,Z)-	71.563	$C_{18}H_{34}O$	266.462		0.07	
75	(-)-Myrtenol	72.087	$C_{10}H_{16}O$	152.2334	Mono	0.15	
76	n-Pentatriacontane	72.462	$C_{35}H_{72}$	492.9462			0.19
77	Montanyl alcohol	72.767	$C_{28}H_{58}O$	410.7595		0.33	
78	α-Curcumene	73.038	$C_{15}H_{22}$	202.3352	Sesqui		0.15
79	3-Methyloctadecane	73.842	$C_{19}H_{40}$	268.5209			0.03
80	Octadecyl chloride	74.477	$C_{18}H_{37}Cl$	288.939		0.63	
81	Nonacosane	75.547	$C_{29}H_{60}$	408.7867	Alkane		0.38
82	n-Octadecyl chloride;	76.096	$C_{18}H_{37}Cl$	288.939		0.04	
83	Octadeamethyl-cyclononasiloxane	77.732	$C_{18}H_{54}O_9Si_9$	667.3855			1.17
84	n-Nonacosane	78.098	$C_{29}H_{60}$	408.7867	Alkane	2.84	
85	n-Octacosane	78.668	$C_{28}H_{58}$	394.7601	Alkane	0.08	
86	n-Nonacosane	79.245	$C_{29}H_{60}$	408.7867	Alkane		0.27
	Total % monoterpene	0.99	0.13	667.3855			0.65
	Total % sesquiterpene	0.33	2.8	320.5093		0.24	
	Total % diterpene	7.55	41.72	667.3855			0.05
	Total % triterpene		0.43	266.4189		0.7	
	Total % ester	0.49	0.15	410.718	Tri		0.43
	Total % of Alkane	4.74	2.4	296.5741			0.05
	Total % of fatty acid.	13.99	40.17	667.3855			0.79

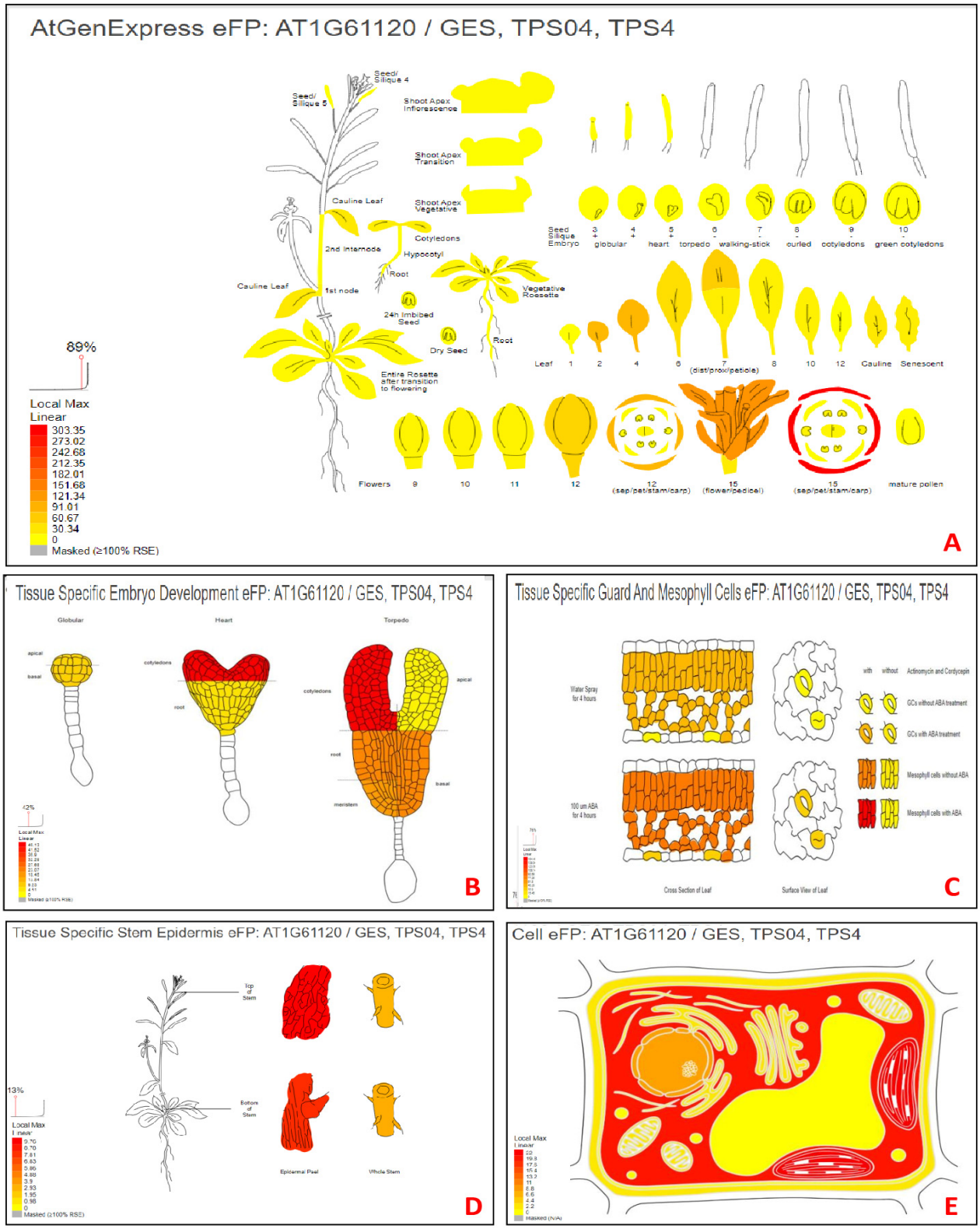

Figure 4. Visualization of the putative "Electronic Fluorescent Pictograph" browsers for exploring the putative tissue expression and cell localization of *SgGES* (AT1G61120) gene based on Arabidopsis gene expression and protein localization at different tissues and cell organs. (**A**) Expression data for different tissues from seedling to flowering stages. (**B**) Expression data for tissue-specific embryo development. (**C**) Expression data for tissue-specific guard and mesophyll cells. (**D**) Expression data for tissue-specific stem epidermis at top and bottom. (**E**) Expression data for different cell organs. The color box represents the expression scale (the more intense the red color, the more gene expression).

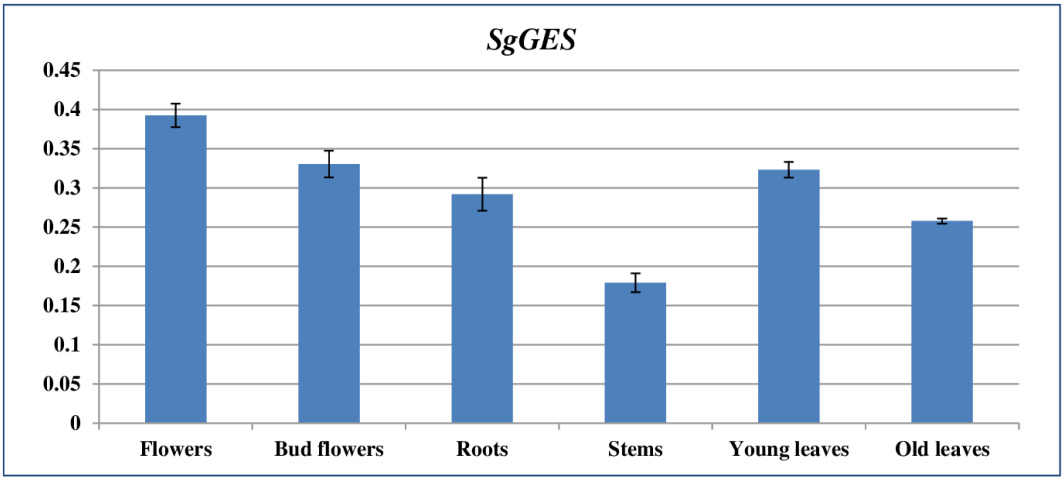

Figure 5. Quantitative RT-PCR validation of expression of *SgGES* gene from *S.guaranitica*. Total RNAs were extracted from young leaves, stems, old leaves, roots, flowers, and bud flower samples and the expression of *SgGES* gene was analyzed using quantitative real-time PCR. *SgACTIN* was used as the internal reference. The values are means ± SE of three biological replicates.

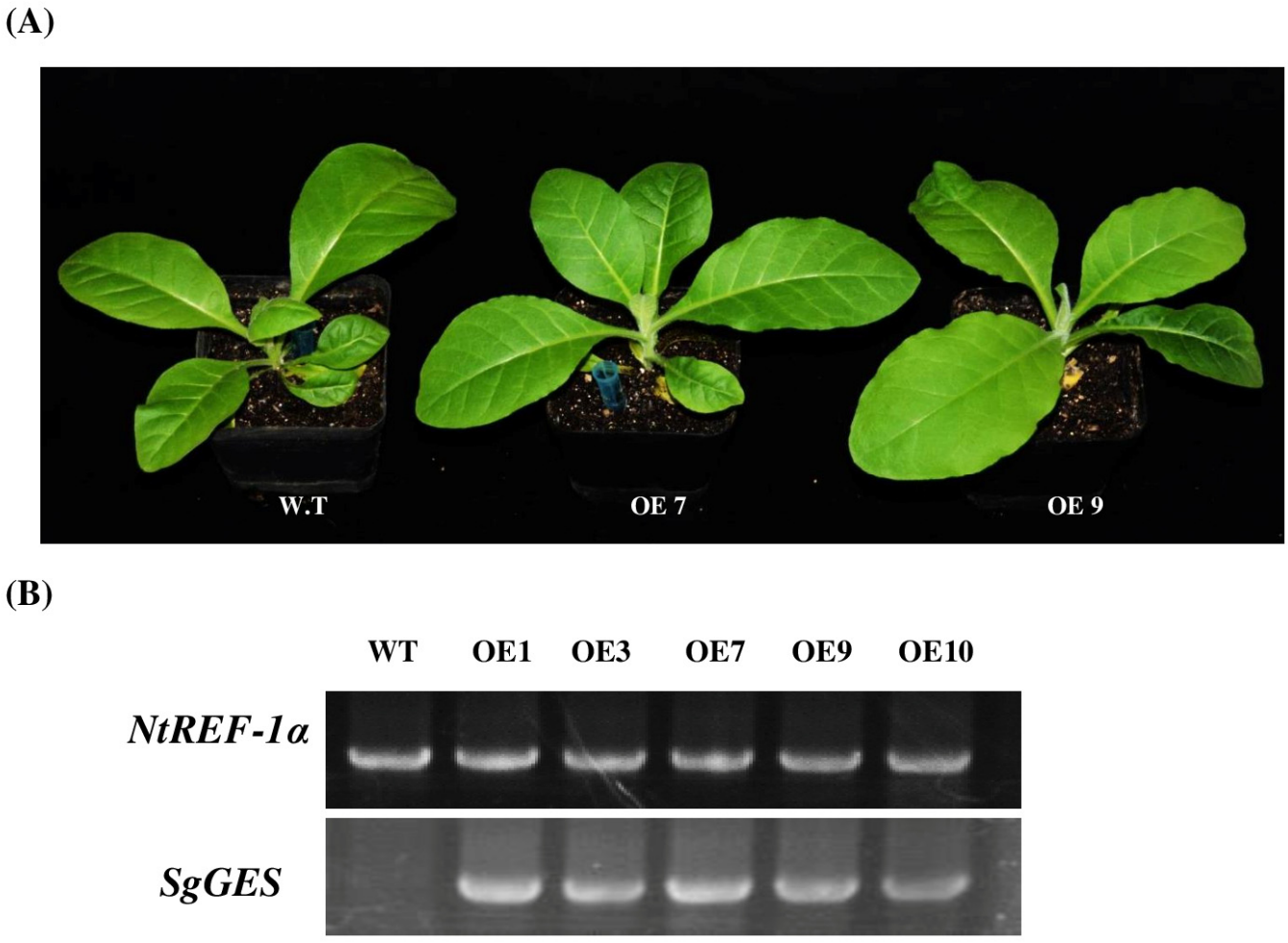

Figure 6. Overexpression of *SgGES* gene in transgenic *N. tabacum*. (**A**) Comparison of the phenotypes of the transgenic *N. tabacum* and wild-type *N. tabacum*. (**B**) Semiquantitative RT-PCR to confirm the expression of terpenoid genes.

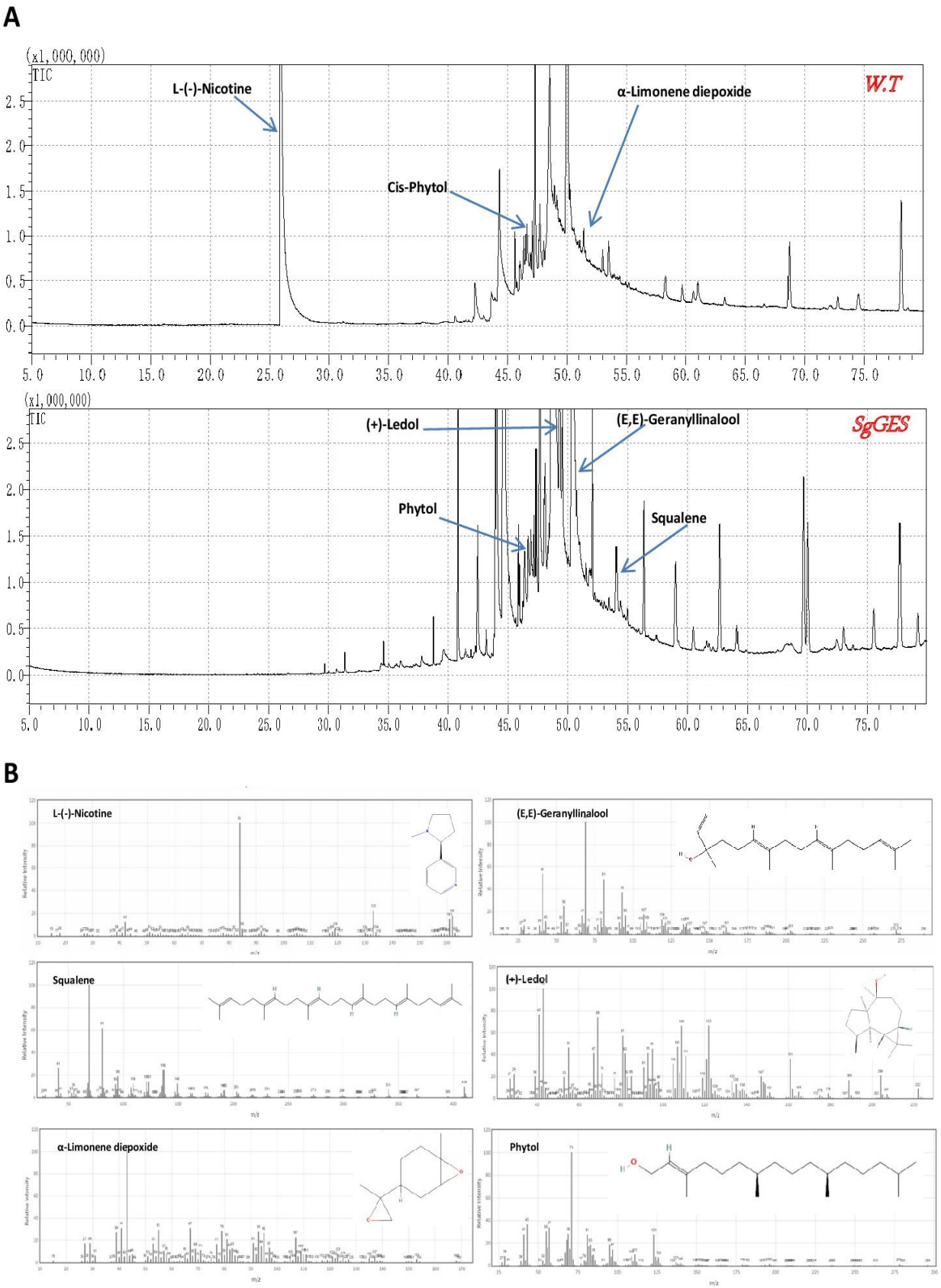

Figure 7. GC-MS mass analysis for terpenoids from non-transgenic and transgenic *N. tabacum*. (**A**) GC-MS peaks of the terpenoids and (**B**) mass spectra of GC peaks with retention time for the major compounds.

4. Discussion

4.1. Cloning and Sequence Analysis of SgGES Gene from S. guaranitica

The *SgGES* gene was identified, and its full-length cDNA was obtained from the leaves of *S. guaranitica* by utilizing a conserved sequence that is remarkably similar to the sequences found in other plant species, including those identified in our query. The full-length cDNA of the *SgGES* gene was acknowledged and isolated from the leaves of *S. guaranitica* based on the conserved sequence, which is highly similar to our query sequence and the other sequences identified in different plant species, including *Salvia splendens*, *Salvia hispanica*, *Salvia miltiorrhiza*, *Prunella vulgaris*, *Handroanthus impetiginosus*, *Leonurus japonicus*, and *Eremophila drummondii*.

When contrasted with diterpene and other terpene synthases, the SgGES protein comprises five domains, which have been identified and designated by the Superfamily, Pfam, and InterPro databases. The first two domains are the terpenoid cyclases/protein prenyltransferase alpha-alpha toroid (IPR008930/SSF48239, from 35 to 133 and IPR008930/SSF48239, from 235 to 440), and the third is the isoprenoid synthase domain (IPR008949/SSF48576, from 463 to 783), while the other domains are terpene synthase N-terminal domain (IPR001906/PF01397, from 226 to 425) and terpene synthase metal-binding domain (IPR005630/PF03936, from 466 to 727) (Figure 2). The putative *SgGES* protein sequence showed various highly conserved domains that are responsible for coordinating the binding between divalent metal ion co-factors and substrate [2,4,12,40,41,44–46], (Figure 2). Furthermore, they are well known for their capacity to bind a tri-nuclear-magnesium cluster, two magnesium ions, and one magnesium ion [12,45,47]. This magnesium cluster binds and interacts with the diphosphate moiety of Geranylgeranyl diphosphate (GFPP) and FPP to catalyze the C20-substrate GGPP and C15-substrate FPP formation [12,40,41,46,48–50]. Finally, the terpene synthase family of proteins consistently includes one or two conserved domains [2,4,9,51]. To further uncover the evolutionary relations between *SgGES* and other plant terpene synthase genes, we used the neighbor-joining method parameters, which generated an evolutionary tree. The classification results pointed to the placement of the *SgGES* protein in the TPS-a subfamily, which is known to encode mono-, sesqui-, and diterpenes. The capacity of *SgGES* to generate diverse types of terpenes has been previously highlighted by [2,4] (Figure 3).

4.2. Putative Tissue Expression Pattern and Subcellular Localizations of SgGES Gene

To uncover the physiological functions of *SgGES*, we screened its putative expression patterns in 72 tissues. The high similarity between *SgGES* and the AT1G61120 gene from *A. thaliana* facilitated this process. The presence of *SgGES* in the tested tissues aligns with the findings of Ali et al. [2,4,9,29], who reported that most TPS genes (e.g., *SoFLDH*, *SgTPSV*, *SoTPS3*, *SgGERIS*, *SoLINS2*, *GmTPS21*, *SoTPS4*, *SgFARD*, *SoNEOD*, and *SoHUMS*) from *S. officinalis*, *Glycine max*, and *S. guaranitica* exhibited high expression levels in various tissues and developmental stages, particularly in flowers, roots, leaves, stems, and seeds. Moreover, the putative subcellular localization for the SgGES protein revealed that our target gene is predominantly present in the cytosol, followed by the plastids, mitochondria, and nuclei. These results align with the findings of Wang et al., Ali et al., Chen et al., and Makhadmeh et al. [2,4,9,31,32,52,53], who reported that numerous TPS genes exhibited clear localization in the plastids, mitochondria, and nuclei (Figure 4E).

4.3. Analysis of SgGES Gene Expression via qRT-PCR

Our study involved the use of qRT-PCR to assess the expression levels of the *SgGES* gene in different tissues. The qPCR data showed that it is most abundant in flowers, followed by flowering buds, young leaves, roots, old leaves, and stems. These findings are congruent with previous studies, which have reported high expression of TPS synthesis genes in flowers, young leaves, bud flowers, roots, old leaves, and stems [2,4,54,55]. The expression of the *SgGES* gene in stems is believed to be influenced by several factors. These factors may include gene-regulatory mechanisms that control post-transcriptionally

and/or post-translationally (Figure 5). Additionally, the expression levels of *SgGES* might be related to tissue developmental stages, which greatly influence the expression of terpene synthase in *Salvia* [2,4,54,55] (Figure 5).

4.4. N. tabacum Plant Phenotypes and Terpene Profile Were Altered by Overexpression of the SgGES Gene

The role of *SgGES* in *N. tabacum* plants was investigated by introducing an overexpression vector pB2GW7-SgGES into *Nicotiana* plants using *Agrobacterium*. We validated the expression of our target gene in the positive transgenic *N. tabacum* plants via sqRT-PCR (Figure 6B). The transgenic lines exhibited a higher expression level of the *SgGES* gene expression when compared to the wild type, thus confirming the presence of the target gene. In the following step, some transgenic plants were chosen (named OE-SgGES -7, OE-SgGES-9, and OE-SgGES-10) for terpene analysis. The results of the morphological analysis indicated that the transgenic plants displayed an accelerated rate of leaf growth in comparison to the wild-type plants (Figure 6A). These results are consistent with the research conducted by Ali et al. [2,4,35], which demonstrated that in *A. thaliana* and *N. tabacum*, overexpression of genes involved in TPS synthesis and terpenoid biosynthesis (*SgGPS*, *SgLINS*, *SgFPPS*, *SoTPS3*, *SoTPS6*, *SoCINS*, *SoLINS*, *SoFLDH*, *SoSABS*, *SoTPA4*, *SgGPS*, and *SoNEOD*) from *S. guaranitica* and *S. officinalis* resulted in enhanced growth and augmented flower development compared to wild-type plants. The reason behind the superiority of transgenic plants with our terpene gene at the levels of growth and development compared with control plants is because of the roles of various terpenes and terpenoids in various metabolic pathways, such as the biosynthesis of terpenoids and steroids; KEGG:map01062, plant secondary metabolites; KEGG:map01060, ubiquinone and other terpenoid–quinone biosynthesis; KEGG:map00130 and biosynthesis of plant hormones; and KEGG:map01070 [56]. Several genes belonging to the TPS family were found to be important in various cell-specific processes, including the synthesis of thalianol as a mono-, sesqui-, di-, and triterpenes; 1,8-cineole; Z-γ-bisabolene; Rhizathalene; and β-amyrin [57–64]. This means that these genes can co-express initially in diverse cells, tissues, and organs to produce a different plant phenotype, hence confirming the role of TPS genes in plant growth, flowering, and development [57–64].

It was essential to analyze the metabolic profiles of tobacco plants after introducing the *SgGES* gene to identify the specific terpenes, and for this purpose, a GC-MS system was employed. The mono-, sesqui-, di-, and triterpene peaks were easily visible; the amount of each component was represented by the percentage of peak area (% peak area). To recognize those terpenes in our transgenic tobacco plants, the libraries of mass spectra from wild-type tobacco extracts were used as a reference. The data presented in Figure 7 and Table 2 unequivocally demonstrate a significant modification in the transgenic plants as a novel peak at the retention time of 50.461 was detected. This peak was identified as (E,E)-geranyllinalool based on the matched mass with the Wiley GC/MS Library, NIST Library, and VOC Analysis S/W software. On the other hand, the production of terpenes by the overexpression of terpene synthase genes in tobacco was described formerly by [2,41,51]. Diverse terpene synthase genes have been identified as capable of producing multiple compounds simultaneously, such as carene, (±)-linalool, cineole, myrcene, β-amyrin, and terpinolene synthases [11,12,65–69]. Based on our perspective, *SgGES* plays a pivotal part in the synthesis of (E,E)-geranyllinalool via the diterpenoid biosynthesis pathway, which is a prominent feature of diterpene biosynthesis processes.

5. Conclusions

S. guaranitica is a valuable Chinese medicinal herb with distinctive pharmacological effects. As a result, cloning and characterizing several genes involved in secondary metabolic pathways will help metabolic engineering of *S. guaranitica* and other therapeutic plants. In this investigation, we cloned the *SgGES* gene as a plant geranyllinalool biosynthetic from *S. guaranitica*. *SgGES* overexpression in *N. tabacum* enhanced leaf formation in the OE-SgGES-

7 and OE-SgGES-9 transgenic lines. In comparison to control plants, these previous lines produced a high amount of (E,E)-geranyllinalool. The presence of (E,E)-geranyllinalool in these transgenic lines demonstrates that *N. tabacum* plants may synthesize the same product via the common mevalonate pathway (MVK) of diterpene biosynthesis, emphasizing the potential role of this gene in producing various types of terpenes, particularly the diterpene (E,E)-geranyllinalool. This study showed that the diterpene gene could be studied using the *N. tabacum* plant as a model plant, which can be used to improve the essential oil composition in *S. guaranitica* and other species via metabolic engineering.

Supplementary Materials: The following supporting information can be downloaded at: https://www.mdpi.com/article/10.3390/horticulturae10070668/s1, Table S1. Expression data for different tissues from seedling to flowering stages, specific embryo development, specific guard and mesophyll cells, and specific stem epidermis at top and bottom. Figure S1. *SgGES*-OE construct used to transform *N. tabacum* plant.

Author Contributions: Conceptualization, J.Z. and M.A.; Gene cloning and plasmid construction steps, A.A.A. (Ahmed Ali Abdelhameed), M.A.E., R.I.E.-k. and F.A.S.; Plant tissue culture and tobacco transformation, M.A.E. and M.A.; qRT-PCR and semi-quantitative RT-PCR (sqRT-PCR) analyses and bioinformatics analyses, A.A.A. (Amal Ahmed Alyamani), H.M.A., M.M.M. and D.B.E.D.; Terpenoid extraction and GC-MS analysis, M.Z., D.B.E.D. and A.H.A.A.; formal analysis, A.H.A.A.; investigation, M.Z.; writing—original draft preparation, J.Z. and M.A.; writing—review and editing, A.A.A. (Ahmed Ali Abdelhameed), H.M.A., M.M.M. and D.B.E.D.; visualization, F.A.S. and M.Z. All authors have read and agreed to the published version of the manuscript.

Funding: The research was funded by Taif University, Saudi Arabia, Project No. (TU-DSPP-2024-213).

Data Availability Statement: All data generated or analyzed during this study are included in this published article and its Supplementary Information Files. The datasets used and/or analyzed during the current study are available from the corresponding author on reasonable request.

Acknowledgments: The authors extend their appreciation to Taif University, Saudi Arabia, for supporting this work through project number (TU-DSPP-2024-213), Desert Research Center (DRC), Egypt.

Conflicts of Interest: The authors declare that the research was conducted in the absence of any commercial or financial relationships that could be construed as a potential conflict of interest.

References

1. Alziar, G. Catalogue Synonymique des Salvia L. Dumonde (Lamiaceae). I.–VI. Biocosme Mesogéen. (1988–1993), 5 (3–4): 87–136; 6(1–2, 4): 79–115, 163–204; 7(1–2): 59–109; 9(2–3): 413–497; 10(3–4): 33–117. Available online: https://www.researchgate.net/publication/288010566_Catalogue_synonymique_des_Salvia_L_du_monde_Lamiaceae_I-VI (accessed on 16 June 2024).
2. Ali, M.; Li, P.; She, G.; Chen, D.; Wan, X.; Zhao, J. Transcriptome and metabolite analyses reveal the complex metabolic genes involved in volatile terpenoid biosynthesis in garden sage (*Salvia officinalis*). *Sci. Rep.* **2017**, *7*, 16074. [CrossRef] [PubMed]
3. Sarrou, E.; Ioannis, G.; Aliki, X.; Domenico, M.; Stefan, M.; Panagiotis, M.; Athanasios, M.; Paschalina, C. Genetic diversity and metabolic profile of *Salvia officinalis* populations: Implications for advanced breeding strategies. *Planta* **2017**, *246*, 201–215. [CrossRef] [PubMed]
4. Ali, M.; Hussain, R.M.; Rehman, N.U.; She, G.; Li, P.; Wan, X.; Guo, L.; Zhao, J. De novo transcriptome sequencing and metabolite profiling analyses reveal the complex metabolic genes involved in the terpenoid biosynthesis in Blue Anise Sage (*Salvia guaranitica* L.). *DNA Res.* **2018**, *25*, 597–617. [CrossRef] [PubMed]
5. Li, D.; Shao, F.; Lu, S. Identification and characterization of mRNA-like noncoding RNAs in *Salvia miltiorrhiza*. *Planta* **2015**, *241*, 1131–1143. [CrossRef] [PubMed]
6. Khater, R. Evaluating the productivity of *Salvia officinalis*, plants using of fertilizers and spraying with vitamins. *Egypt. J. Desert Res.* **2022**, *72*, 47–71. [CrossRef]
7. Zhenqing, B.; Wenrui, L.; Yanyan, J.; Zhiyong, Y.; Jie, J.; Wenli, H.; Pengguo, X.; Zongsuo, L. The ethylene response factor SmERF6 co-regulates the transcription of SmCPS1 and SmKSL1 and is involved in tanshinone biosynthesis in *Salvia miltiorrhiza* hairy roots. *Planta* **2018**, *248*, 243–255.
8. Bohlmann, J.; Meyer-Gauen, G.; Croteau, R. Plant terpenoid synthases: Molecular biology and phylogenetic analysis. *Proc. Natl. Acad. Sci. USA* **1998**, *95*, 4126–4133. [CrossRef] [PubMed]
9. Ali, M.; Alshehri, D.; Alkhaibari, A.M.; Elhalem, N.A.; Darwish, D.B.E. Cloning and Characterization of 1,8-Cineole Synthase (*SgCINS*) Gene From the Leaves of *Salvia guaranitica* plant. *Front. Plant Sci.* **2022**, *13*, 869432. [CrossRef]

10. Ali, M.; Nishawy, E.; Ramadan, W.A.; Ewas, M.; Rizk, M.S.; Sief-Eldein, A.G.M.; El-Zayat, M.A.S.; Hassan, A.H.M.; Guo, M.; Hu, G.W.; et al. Molecular characterization of a Novel NAD+-dependent farnesol dehydrogenase *SoFLDH* gene involved in sesquiterpenoid synthases from *Salvia officinalis*. *PLoS ONE* **2021**, *17*, e0269045. [CrossRef]
11. Xi, J.; Rossi, L.; Lin, X.; Xie, D.Y. Overexpression of a synthetic insect–plant geranyl pyrophosphate synthase gene in *Camelina sativa* alters plant growth and terpene biosynthesis. *Planta* **2016**, *244*, 215–230. [CrossRef]
12. Abbas, F.; Ke, Y.; Yu, R.; Fan, Y. Functional characterization and expression analysis of two terpene synthases involved in floral scent formation in *Lilium* 'Siberia'. *Planta* **2019**, *249*, 71–93. [CrossRef] [PubMed]
13. Wallach, O. Zur KentniB der Terpene uDd dec atherischen Oele. *Liebig's Ann. Chern.* **1887**, *239*, 1–54. [CrossRef]
14. Ruzicka, L. The isoprene rule and the biogenesis of terpenic compounds. *Experientia* **1953**, *9*, 357–367. [CrossRef]
15. Ruzicka, L. Faraday Lecture (History of the isoprene rule). *Proc. Chern. Soc.* **1959**, 341–360.
16. Ruzicka, L. In the borderland between bioorganic chemistry and biochemistry. *Annu. Rev. Biochem.* **1973**, *42*, 1–20. [CrossRef] [PubMed]
17. Trapp, S.; Croteau, R. Defensive resin biosynthesis in conifers. *Annu. Rev. Plant Physiol. Plant Mol. Biol.* **2001**, *52*, 689–724. [CrossRef] [PubMed]
18. Gershenzon, J.; Kreish, W. Biochemistry of terpenoids: Monoterpenes, sesquiterpenes, diterpenes, sterols, cardiac glycosides and steroid saponins. In *Biochemistry of Plant Secondary Metabolism*; Wink, M., Ed.; CRC Press: Boca Raton, FL, USA, 1999; pp. 222–299.
19. Dorothea, T.; Wilhelm, B.; Armin, H.; Francesco, L.; Ursula, S.R.R.; Jörg-Peter, S. Practical approaches to plant volatile analysis. *Plant J.* **2006**, *45*, 540–560.
20. Ali, M.; Miao, L.; Hou, Q.; Darwish, D.B.; Alrdahe, S.S.; Ali, A.; Benedito, V.A.; Tadege, M.; Wang, X.; Zhao, J. Overexpression of Terpenoid Biosynthesis Genes From Garden Sage (*Salvia officinalis*) Modulates Rhizobia Interaction and Nodulation in Soybean. *Front. Plant Sci.* **2021**, *12*, 783269. [CrossRef] [PubMed]
21. Ali, M.; Miao, L.; Soudy, F.A.; Darwish, D.B.E.; Alrdahe, S.S.; Alshehri, D.; Benedito, V.A.; Tadege, M.; Wang, X.; Zhao, J. Overexpression of Terpenoid Biosynthesis Genes Modifies Root Growth and Nodulation in Soybean (*Glycine max*). *Cells* **2022**, *11*, 2622. [CrossRef]
22. Makris, D.P.; Boskou, G.; Andrikopoulos, N.K. Polyphenolic Content and in Vitro Antioxidant Characteristics of Wine Industry and other Agri-Food Solid Waste Extracts. *J. Food Compos. Anal.* **2007**, *20*, 125–132. [CrossRef]
23. Aziz, R.A.; Hamed, F.K.; Abdulah, N.A. Determination of the main components of the essential oil extracted from *Salvia fruticosa* by sing GC and GC-MS DAMASCUS. *J. Agric. Sci.* **2008**, *24*, 223–236.
24. Loizzo, M.R.; Menichini, F.; Tundis, R.; Bonesi, M.; Nadjafi, F.; Saab, A.M.; Frega, N.G.; Menichini, F. Comparative chemical composition and antiproliferative activity of aerial parts of *Salvia leriifolia Benth*. And *Salvia acetabulosa* L. essential oils against human tumor cell in vitro models. *J. Med. Food* **2010**, *13*, 62–69. [PubMed]
25. Atsuko, T.; Hiroshi, O. Phylogenetic relationships among subgenera, species, and varieties of *Japanese Salvia* L. (Lamiaceae). *J. Plant Res.* **2011**, *124*, 245–252.
26. Hua, W.P.; Zhang, Y.; Song, J.; Zhao, L.J.; Wang, Z.Z. *De novo* transcriptome sequencing in *Salvia miltiorrhiza* to identify genes involved in the biosynthesis of active ingredients. *Genomic* **2011**, *98*, 272–279.
27. Nadaf, M.; Nasrabadi, M.; Halimi, M. GC-MS analysis of n-hexane extract from aerial parts of *Salvia nemorosa*. *Middle-East J. Sci. Res.* **2012**, *11*, 1127–1130.
28. Fateme, A.M.; Mohammad, H.F.; Abdolhossein, R.; Ali, Z.; Maryam, S. Volatile Constituents of *Salvia compressa* and *Logochilus macranthus*, two Labiatae Herbs Growing wild in Iran. *Res. J. Recent Sci.* **2013**, *2*, 66–68.
29. Ali, M. Cloning, molecular characterization and functional analysis of the CIS-muuroladiene synthase (*SgCMS*) gene from leaves of *Salvia guaranitica* plant. *Egypt. J. Desert Res.* **2023**, *73*, 239–263. [CrossRef]
30. Mehmood, N.; Yuan, Y.; Ali, M.; Ali, M.; Iftikhar, J.; Cheng, C.; Lyu, M.; Wu, B. Early transcriptional response of terpenoid metabolism to *Colletotrichum gloeosporioides* in a resistant wild strawberry *Fragaria nilgerrensis*. *Phytochemistry* **2021**, *181*, 112590. [CrossRef] [PubMed]
31. Makhadmeh, I.M.; Thabet, S.G.; Ali, M.; Alabbadi, B.; Albalasmeh, A.; Alqudah, A.M. Exploring genetic variation among Jordanian Solanum lycopersicon L. landraces and their performance under salt stress using SSR markers. *J. Genet. Eng. Biotechnol.* **2022**, *20*, 45. [CrossRef]
32. Makhadmeh, I.; Albalasmeh, A.A.; Ali, M.; Thabet, S.G.; Darabseh, W.A.; Jaradat, S.; Alqudah, A.M. Molecular Characterization of Tomato (*Solanum lycopersicum* L.) Accessions under Drought Stress. *Horticulturae* **2022**, *8*, 600. [CrossRef]
33. Hussain, R.M.; Ali, M.; Feng, X.; Li, X. The essence of NAC gene family to the cultivation of drought-resistant soybean (*Glycine max* L. Merr.) cultivars. *BMC Plant Biol.* **2017**, *17*, 55. [CrossRef]
34. Horsch, R.B.; Fraley, R.T.; Rogers, S.G.; Sanders, P.R.; Lloyd, A.; Hoffmann, N. Inheritance of functional foreign genes in plants. *Science* **1984**, *223*, 496–498. [CrossRef] [PubMed]
35. Lloyd, A.M.; Barnason, A.R.; Rogers, S.G.; Byrne, M.C.; Fraley, R.T.; Horsch, R.B. Transformation of Arabidopsis thaliana with *Agrobacterium tumefaciens*. *Science* **1986**, *234*, 464–466. [CrossRef] [PubMed]
36. Burow, M.D.; Chlan, C.A.; Sen, P.; Lisca, A.; Murai, N. High-frequency generation of transgenic tobacco plants after modified leaf disk cultivation with Agrobacterium tumefaciens. *Plant Mol. Biol. Rep.* **1990**, *8*, 124–139. [CrossRef]

37. Wise, M.L.; Savage, T.J.; Katahira, E.; Croteau, R. Monoterpene synthases from common sage (*Salvia officinalis*) cDNA isolation, characterization, and functional expression of (+)-sabinene synthase, 1,8-cineole synthase, and (+)-bornyl diphosphate synthase. *J. Biol. Chem.* **1998**, *273*, 14891–14899. [CrossRef]
38. Anders, S.; Huber, W. Differential expression analysis for sequence count data. *Genome Biol.* **2010**, *11*, R106. [CrossRef]
39. Rehman, N.U.; Ali, M.; Ahmad, M.Z.; Liang, G.; Zhao, J. Strigolactones promote rhizobia interaction and increase nodulation in soybean (*Glycine max*). *Microb Pathog.* **2017**, *114*, 420–430. [CrossRef] [PubMed]
40. Degenhardt, J.; Köllner, T.G.; Gershenzon, J. Monoterpene and sesquiterpene synthases and the origin of terpene skeletal diversity in plants. *Phytochemistry* **2009**, *70*, 1621–1637. [CrossRef]
41. Su-Fang, E.; Mohamed-Hussein, Z.A.; Othman, R.; Shaharuddin, N.A.; Ismail, I.; Zainal, Z. Functional Characterization of Sesquiterpene Synthase from *Polygonum minus*. *Sci. World J.* **2014**, *2014*, 840592. [CrossRef]
42. Jiang, S.Y.; Jin, J.; Sarojam, R.; Ramachandran, S. A Comprehensive Survey on the Terpene Synthase Gene Family Provides New Insight into Its Evolutionary Patterns. *Genome Biol. Evol.* **2019**, *11*, 2078–2098. [CrossRef]
43. Yan, X.M.; Zhou, S.S.; Liu, H.; Zhao, S.W.; Tian, X.C.; Shi, T.L.; Bao, Y.T.; Li, Z.C.; Jia, K.H.; Nie, S.; et al. Unraveling the evolutionary dynamics of the TPS gene family in land plants. *Front. Plant Sci.* **2023**, *14*, 1273648. [CrossRef] [PubMed]
44. López-Gallego, F.; Wawrzyn, G.T.; Schmidt-Dannert, C. Selectivity of fungal sesquiterpene synthases: Role of the active site's H-1α loop in catalysis. *Appl. Environ. Microbiol.* **2010**, *76*, 7723–7733. [CrossRef] [PubMed]
45. Lima, A.S.; Jette, S.; Brigitte, L.; Johannes, N.; Jose, G.B.; Figueiredo, A.C.; Luis, G.P.; Jo, D.; Helena, T. Genomic characterization, molecular cloning and expression analysis of two terpene synthases from *Thymus caespititius* (Lamiaceae). *Planta* **2013**, *238*, 191–204. [CrossRef] [PubMed]
46. Rebecca, S.W.; Ayelign, M.A.; Lina, B.; Elaheh, N.; Soheil, S.M. Cloning and functional characterization of a floral repressor gene from *Lavandula Angustifolia*. *Planta* **2020**, *251*, 41.
47. Christianson, D.W. Structural biology and chemistry of the terpenoid cyclases. *Chem. Rev.* **2006**, *106*, 3412–3442. [CrossRef] [PubMed]
48. Davis, E.M.; Croteau, R. Cyclization enzymes in the biosynthesis of monoterpenes, sesquiterpenes, and diterpenes. In *Biosynthesis: Aromatic Polyketides, Isoprenoids, Alkaloids*; Vederas, J.C., Leeper, F.J., Eds.; Springer: Berlin, Germany, 2000; pp. 53–95.
49. Whittington, D.A.; Wise, M.L.; Urbansky, M.; Coates, R.M.; Croteau, R.B.; Christianson, D.W. Bornyl diphosphate synthase: Structure and strategy for carbocation manipulation by a terpenoid cyclase. *Proc. Natl. Acad. Sci. USA* **2002**, *99*, 15375–15380. [CrossRef] [PubMed]
50. Hyatt, D.C.; Youn, B.; Zhao, Y.; Santhamma, B.; Coates, R.M.; Croteau, R.B.; Kang, C. Structure of limonene synthase, a simple model for terpenoid cyclase catalysis. *Proc. Natl. Acad. Sci. USA* **2007**, *104*, 5360–5365. [CrossRef] [PubMed]
51. El-ramah, F.; Ali, M.; Elsherbeny, E.; Ahmed, M. Molecular cloning and characterization of beta-amyrin synthase (*SoAMYS*) gene from *Salvia officinalis* plant. *Egypt. J. Desert Res.* **2022**, *72*, 27–45. [CrossRef]
52. Wang, B.; Sun, W.; Li, Q.; Li, Y.; Luo, H.; Song, J.; Sun, C.; Qian, J.; Zhu, Y.; Hayward, A.; et al. Genome-wide identification of phenolic acid biosynthetic genes in *Salvia miltiorrhiza*. *Planta* **2015**, *241*, 711–725. [CrossRef]
53. Chen, X.; Chen, H.; Yuan, J.S.; Köllner, T.G.; Chen, Y.; Guo, Y.; Zhuang, X.; Chen, X.; Zhang, Y.J.; Fu, J.; et al. The rice terpene synthase gene *OsTPS19* functions as an (S)-limonene synthase in planta, and its overexpression leads to enhanced resistance to the blast fungus *Magnaporthe oryzae*. *Plant Biotechnol. J.* **2018**, *16*, 1778–1787. [CrossRef]
54. Croteau, R.; Felton, M.; Karp, F.; Kjonaas, R. Relationship of camphor biosynthesis to leaf development in sage *Salvia officinalis*. *Plant Physiol.* **1981**, *67*, 820–824. [CrossRef] [PubMed]
55. Sabine, G.-G.; Corinna, S.; Ralf, S.; Johannes, N. Seasonal influence on gene expression of monoterpene synthases in *Salvia officinalis* (Lamiaceae). *J. Plant Physiolol.* **2012**, *169*, 353–359.
56. Abeed, A.H.A.; Ali, M.; Ali, E.F.; Majrashi, A.; Eissa, M.A. Induction of *Catharanthus roseus* Secondary Metabolites When *Calotropis procera* Was Used as Bio-Stimulant. *Plants* **2021**, *10*, 1623. [CrossRef]
57. Chen, F.; Ro, D.K.; Petri, J.; Gershenzon, J.; Bohlmann, J.; Pichersky, E.; Tholl, D. Characterization of a root-specific Arabidopsis terpene synthase responsible for the formation of the volatile monoterpene 1,8-cineole. *Plant Physiol.* **2004**, *135*, 1956–1966. [CrossRef]
58. Ro, D.-K.; Ehlting, J.; Keeling, C.I.; Lin, R.; Mattheus, N.; Bohlmann, J. Microarray expression profiling and functional characterization of *AtTPS* genes: Duplicated *Arabidopsis thaliana* sesquiterpene synthase genes *At4g13280* and *At4g13300* encode root-specific and wound-inducible (Z)-γ-bisabolene synthases. *Arch. Biochem. Biophys.* **2006**, *448*, 104–116. [CrossRef]
59. Kampranis, S.C.; Ioannidis, D.; Purvis, A.; Mahrez, W.; Ninga, E.; Katerelos, N.A.; Anssour, S.; Dunwell, J.M.; Degenhardt, J.; Makris, A.M.; et al. Rational conversion of substrate and product specificity in a Salvia monoterpene synthase: Structural insights into the evolution of terpene synthase function. *Plant Cell.* **2007**, *19*, 1994–2005. [CrossRef]
60. Field, B.; Osbourn, A.E. Metabolic diversification–independent assembly of operon-like gene clusters in different plants. *Science* **2008**, *320*, 543–547. [CrossRef] [PubMed]
61. Chen, F.; Tholl, D.; Bohlmann, J.; Pichersky, E. The family of terpene synthases in plants: A mid-size family of genes for specialized metabolism that is highly diversified throughout the kingdom. *Plant J.* **2011**, *66*, 212–229. [CrossRef] [PubMed]
62. Field, B.; Fiston-Lavier, A.S.; Kemen, A.; Geisler, K.; Quesneville, H.; Osbourn, A.E. Formation of plant metabolic gene clusters-swithin dynamic chromosomal regions. *Proc. Natl. Acad. Sci. USA* **2011**, *108*, 16116–16121. [CrossRef]

63. Vaughan, M.M.; Wang, Q.; Webster, F.X.; Kiemle, D.; Hong, Y.J.; Tantillo, D.J.; Coates, R.M.; Wray, A.T.; Askew, W.; O'Donnell, C.; et al. Formation of the unusual semivolatile diterpene rhizathalene by the Arabidopsis class I terpene synthaseTPS08 in the root stele is involved in defense against belowground herbivory. *Plant Cell* **2013**, *25*, 1108–1125. [CrossRef]
64. Wang, Q.; Jia, M.; Huh, J.H.; Muchlinski, A.; Peters, R.J.; Tholl, D. Identification of a Dolabellane Type Diterpene Synthase and other Root-Expressed Diterpene Synthases in Arabidopsis. *Front. Plant Sci.* **2016**, *7*, 1761. [CrossRef] [PubMed]
65. Lücker, J.; El Tamer, M.K.; Schwab, W.; Verstappen, F.W.; van der Plas, L.H.; Bouwmeester, H.J.; Verhoeven, H.A. Monoterpene biosynthesis in lemon (*Citrus limon*). cDNA isolation and functional analysis of four monoterpene synthases. *Eur. J. Biochem.* **2002**, *269*, 3160–3171. [CrossRef] [PubMed]
66. Faldt, J.; Martin, D.; Miller, B.; Rawat, S.; Bohlmann, J. Traumatic resin defense in Norway spruce (*Picea abies*): Methyl jasmonate-induced terpene synthase gene expression, and cDNA cloning and functional characterization of (+)-3-carene synthase. *Plant Mol. Biol.* **2003**, *51*, 119–133. [CrossRef] [PubMed]
67. Yoko, I.; David, R.G.; Eyal, F.; Efraim, L.; Eran, P. Characterization of Geraniol Synthase from the Peltate Glands of Sweet Basil. *Plant Physiol.* **2004**, *134*, 370–379.
68. Shimada, T.; Endo, T.; Fujii, H.; Hara, M.; Omura, M. Isolation and characterization of (E)-beta-ocimene and 1,8 cineole synthases in *Citrus unshiu* Marc. *Plant Sci.* **2005**, *168*, 987–995. [CrossRef]
69. Fahnrich, A.; Krause, K.; Piechulla, B. Product variability of the 'cineole cassette' monoterpene synthases of related *Nicotiana* species. *Mol. Plant* **2011**, *4*, 965–984. [CrossRef]